Design and Analysis of a Floating-Wind Shallow-Water Mooring System Featuring Polymer Springs

Preprint

Ericka Lozon,[1] Matthew Hall,[1] Paul McEvoy,[2] Seojin Kim,[2] and Bradley Ling[3]

1 National Renewable Energy Laboratory
2 Tfl Marine Ltd.
3 Principle Power Inc.

Presented at International Offshore Wind Technical Conference (IOWTC2022)
Boston, Massachusetts
December 7–8, 2022

NREL is a national laboratory of the U.S. Department of Energy
Office of Energy Efficiency & Renewable Energy
Operated by the Alliance for Sustainable Energy, LLC

This report is available at no cost from the National Renewable Energy Laboratory (NREL) at www.nrel.gov/publications.

Contract No. DE-AC36-08GO28308

Conference Paper
NREL/CP-5000-83342
October 2022

Design and Analysis of a Floating-Wind Shallow-Water Mooring System Featuring Polymer Springs

Preprint

Ericka Lozon,[1] Matthew Hall,[1] Paul McEvoy,[2] Seojin Kim,[2] and Bradley Ling[3]

1 National Renewable Energy Laboratory
2 Tfl Marine Ltd.
3 Principle Power Inc.

Suggested Citation
Lozon, Ericka, Matthew Hall, Paul McEvoy, Seojin Kim, and Bradley Ling. 2022. *Design and Analysis of a Floating-Wind Shallow-Water Mooring System Featuring Polymer Springs: Preprint*. Golden, CO: National Renewable Energy Laboratory. NREL/CP-5000-83342. https://www.nrel.gov/docs/fy23osti/83342.pdf.

NREL is a national laboratory of the U.S. Department of Energy
Office of Energy Efficiency & Renewable Energy
Operated by the Alliance for Sustainable Energy, LLC

This report is available at no cost from the National Renewable Energy Laboratory (NREL) at www.nrel.gov/publications.

Contract No. DE-AC36-08GO28308

Conference Paper
NREL/CP-5000-83342
October 2022

National Renewable Energy Laboratory
15013 Denver West Parkway
Golden, CO 80401
303-275-3000 • www.nrel.gov

NOTICE

This work was authored in part by the National Renewable Energy Laboratory, operated by Alliance for Sustainable Energy, LLC, for the U.S. Department of Energy (DOE) under Contract No. DE-AC36-08GO28308. Funding provided by the National Offshore Wind Research and Development Consortium for the project “Technical Qualification and Commercial Assessment of Innovative Shallow Water Mooring Components for Floating Wind Platforms.” The views expressed herein do not necessarily represent the views of the DOE or the U.S. Government. The U.S. Government retains and the publisher, by accepting the article for publication, acknowledges that the U.S. Government retains a nonexclusive, paid-up, irrevocable, worldwide license to publish or reproduce the published form of this work, or allow others to do so, for U.S. Government purposes.

DESIGN AND ANALYSIS OF A FLOATING-WIND SHALLOW-WATER MOORING SYSTEM FEATURING POLYMER SPRINGS

Ericka Lozon
National Renewable Energy Laboratory
Golden, Colorado, U.S.A.

Matthew Hall
National Renewable Energy Laboratory
Golden, Colorado, U.S.A.

Paul McEvoy
Tfl Marine Ltd
Dublin, Ireland

Seojin Kim
Tfl Marine Ltd
Dublin, Ireland

Bradley Ling
Principle Power Inc
Emeryville, California, U.S.A.

ABSTRACT

This paper presents a mooring system design featuring polymer springs for the VolturnUS-S 15-MW reference floating wind turbine in site conditions for the New York Bight at a 50-m water depth. Polymer springs have a nonlinear stress-strain curve that allows a stiffer response at low loads and a more flexible response at higher loads, potentially reducing peak mooring line tensions. The mooring dynamics model MoorDyn has been extended to model springs with nonlinear tension-strain curves from a user-inputted look-up table. This MoorDyn modeling advancement is verified against OrcaFlex simulation results. Using MoorDyn's updated capabilities, a spring-equipped catenary mooring system is designed for the 15-MW floating system, along with a baseline catenary mooring system that does not use polymer springs. The floating wind turbine simulator OpenFAST is used to simulate the mooring systems in design-driving load cases to show the effect of polymer springs on key dynamic behaviours. The results show that the spring-equipped design reduces peak tensions by up to 60%, whereas the turbine offsets stay within a maximum of 7.2 m, which is still a reasonable offset limit for cable considerations. The reduction in peak tensions results in a significant decrease in damage equivalent loads—on the order of 50% for upwind lines in fully loaded conditions. These results show that polymer springs can effectively reduce peak tensions and fatigue loads in mooring systems at shallow water depths.

Keywords: floating offshore wind, shallow water, mooring system, polymer springs

1. INTRODUCTION

The U.S. offshore wind energy industry has significant potential in areas of intermediate (40–80 m) water depth, where the feasible wind turbine substructure type transitions from fixed bottom to floating [1]. However, the support structure design space has not yet converged to a single optimal technology for these areas. Semisubmersibles are a well-established floating platform configuration but cost-effective mooring design at these shallow depths is difficult [2]. Shallow-water mooring systems are challenged by the need to mitigate against the potential for large tension fluctuations and the risk of snap loads without having an excessively large footprint [3]. Withstanding these loads requires larger mooring components, which increase the costs of the mooring system and its installation.

Previous work on shallow-water mooring systems for floating offshore wind turbines highlights the challenges. Hsu et al. discussed snap loads on mooring lines in water depths ranging from 50 to 300 m [3]. They report that lines with lower pretension have a higher probability of going slack and that these events have a considerable negative impact on the fatigue life. Xu et al. analyzed several mooring designs for the Offshore Code Comparison Collaboration Continuation (OC4) semisubmersible floating wind turbine at a 50-m water depth and found that an all-chain mooring design was not cost effective at this depth due to the heavy chain weight and large tension extremes [4]. Instead, chain-clump-buoy and fibre mooring systems were found to be the most promising from a performance and cost-efficiency standpoint. Huang and Yang analyzed the effect of water depth on mooring system design for depths ranging from 50–100 m [5]. The analysis showed that the 50-m water depth resulted in the heaviest chain, whereas the 100-m water depth resulted in much longer mooring lines. To balance the costs of chain diameter and line length, Huang and Yang found that the 60- to 80-m water depth range minimizes mooring system cost.

Continued research is needed to understand cost reduction techniques for shallow-water mooring systems. One approach is the use of spring elements with nonlinear response curves, acting as a stiffer spring at low loads and showing more flexibility at the mooring system's design tensions. The lower stiffness at design tensions reduces tension oscillations due to wave-induced platform motions with less platform offset than other tension-

mitigation approaches, thereby reducing peak mooring loads and allowing less costly mooring components. Harrold et al. demonstrate a nonlinear spring technology based on a hydraulic mechanism and show through simulations that it can reduce peak loads on a semisubmersible floating wind turbine's mooring system by 10% [6]. McEvoy et al. present a novel fiber spring mooring (FSM) system that comprises a light-weight rope with a polymer-based nonlinear spring device close to the fairlead [7]. The FSM mooring system was modeled in OrcaFlex for water depths of 30-50 m with a catenary mooring system used as a basis for comparison. The results showed that using the FSM could reduce maximum mooring line loads by 37%-63% and mooring footprint by 86%-95%. An example of a mooring line with polymer springs at the fairlead is shown in Figure 1.

In this paper, we explore the effect of including polymer springs in the mooring system of the UMaine VolturnUS-S reference design in a shallow water depth of 50 m. First, a baseline mooring system design is developed by adjusting the original all-chain catenary mooring system of the VolturnUS-S reference design for New York Bight site conditions. Next, a modified mooring system is developed by inserting polymer springs and tuning the spring properties and line length while keeping the same anchor spacing and line diameter. Comparing the two mooring designs helps analyze the effects of polymer springs on key dynamic behaviors of the semisubmersible floating offshore wind turbine.

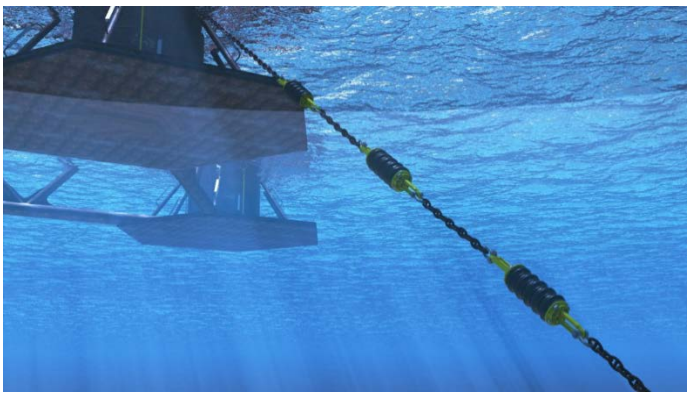

FIGURE 1: SAMPLE RENDERING OF POLYMER SPRINGS ON AN OFFSHORE WIND TURBINE MOORING LINE

2. POLYMER SPRING MODELING

The polymer spring component that we studied in this paper is the SeaSpring developed by TfI Marine. An example of its tension-strain response curve is shown in Figure 2. The spring features a curved, regressive response up until its rated load, at which point the spring's compliance has been exhausted and the tension increases steeply. Properly modeling this nonlinear response is necessary to evaluate the behavior of polymer springs in shallow-water mooring systems. We expanded MoorDyn, the mooring dynamics module used in the floating wind simulator OpenFAST, to model the nonlinear stress-strain curves of polymer spring components. The following sections outline MoorDyn polymer spring modeling and detail the verification process of the MoorDyn advancements.

2.1 Nonlinear Tension-Strain Response Model

To represent a nonlinear tension-strain response in MoorDyn, we departed from the existing linear elasticity model. Mooring line elasticity in MoorDyn is normally represented using a linear tension-strain relation represented by a stiffness coefficient, EA, which is manually specified for each mooring line type. As detailed further in [8], the tension in a line segment is calculated as the product of EA and the segment strain:

$$T = EA\epsilon \tag{1}$$

A nonlinear tension-strain relation can be read from a lookup table, in which case the tension of each segment is linearly interpolated from the lookup table based on the segment strain:

$$T_{interpolated} = f(\epsilon) \tag{2}$$

where f represents the linear interpolation operation. To integrate smoothly with the rest of the elasticity calculations, which expect an EA coefficient, an effective stiffness is calculated from (3):

$$EA = \frac{T_{interpolated}}{\epsilon} \tag{3}$$

for use in (1). This approach makes it easy to switch between linear and nonlinear tension-strain settings.

2.2 MoorDyn Model Verification

We conducted a verification process to ensure that MoorDyn can properly model the nonlinear elasticity of the polymer springs. A representative mooring system featuring polymer springs was set up in both MoorDyn and OrcaFlex. This preliminary mooring design was provided by TFI to demonstrate the performance of the polymer spring in a catenary mooring system located in shallow water. The mooring system features three mooring lines of 117-mm R3-grade studlink chain in a water depth of 65 m. Mooring lines 2 and 3 are about 824 m in length, with an anchor radius of 845 m. The downwind line, mooring line 1, is shorter and spaced more closely with a length of about 725 m and an anchor radius of 801 m. Each line has a 13-m polymer spring with the response curve shown in Figure 2. The polymer springs are separated from the fairlead connection using 10 m of chain.

We used a simple single-line test to verify that MoorDyn captures the full nonlinear tension-strain curve of the polymer spring. This analysis isolates mooring line 1. Using the MoorDyn driver, which allows use independent from OpenFAST, the fairlead of the line was extended 45 m from the starting position at a speed of 0.25 m/s. The graph in Figure 2 plots MoorDyn tension versus strain for segment 1 of the spring line object. The inputted tension-strain curve is also plotted. As shown in the graph, the curve obtained from the MoorDyn simulation is indistinguishable from the user-inputted curve. This closely-matched verification result confirms that MoorDyn accurately captures the nonlinear elasticity of the polymer spring.

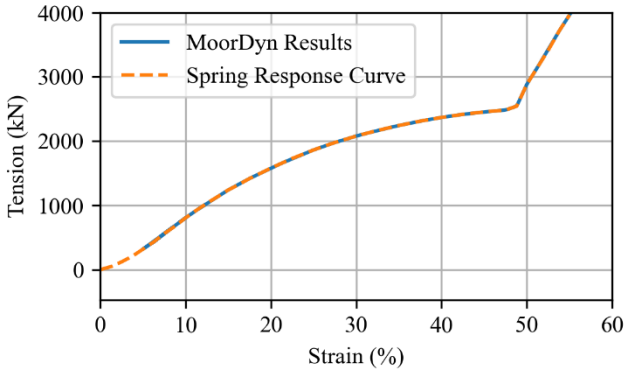

FIGURE 2: POLYMER SPRING TENSION-STRAIN RESPONSE CURVE AND VERIFICATION RESULTS

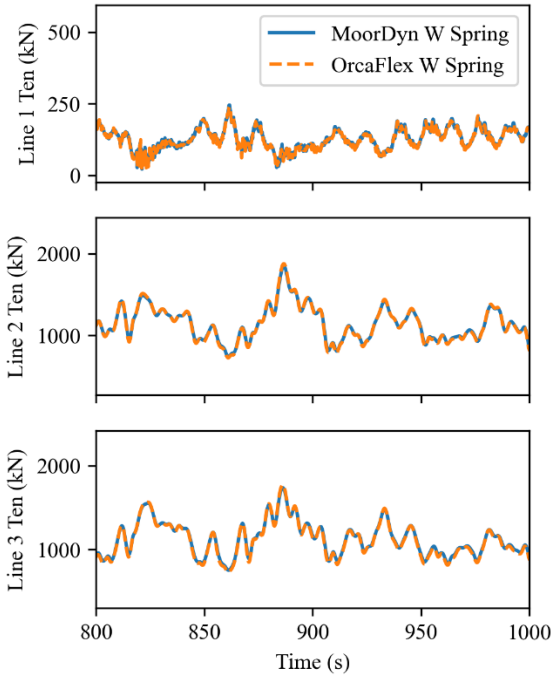

FIGURE 3: RESULTS FROM MOORDYN VERIFICATION WITH ORCAFLEX DATA

To verify MoorDyn's modeling of the polymer spring dynamics within a mooring system, we set up the full three-line mooring system in both MoorDyn and OrcaFlex. The simulations were driven using prescribed motions based on a previous OrcaFlex simulation of a floating wind turbine in 33 m/s wind and 10.1 m H_s waves. Figure 3 plots the tensions of the system's three lines as calculated by MoorDyn and OrcaFlex. The time series plots show close agreement between models. Mooring line 1 shows more tension differences because it is downwind so small differences on the order of 10 kN to 100 kN are more visible. Table 1 shows statistics of the tensions of each line. The mean and maximum tensions are within 2% for all three lines. The persisting small tension differences may be explained by differences in model formulations or discretization levels. Regardless, the closely matched verification result confirms that MoorDyn accurately captures the polymer spring behavior and can be used for the design and analysis of systems that feature polymer springs.

TABLE 1: LINE TENSION STATISTICS IN MOORDYN AND ORCAFLEX FROM VERIFICATION CASE

		OrcaFlex	MoorDyn	% Change
L1 tension (kN)	Mean	140	143	2%
	Std. dev.	46	46	-1%
	Max.	353	353	0%
	Min.	21	17	-19%
L2 tension (kN)	Mean	1079	1082	0%
	Std. dev.	258	245	-5%
	Max.	2043	2002	-2%
	Min.	536	542	1%
L3 tension (kN)	Mean	1076	1087	1%
	Std. dev.	247	236	-4%
	Max.	2120	2086	-2%
	Min.	575	592	3%

3. LOAD CASES AND MOORING SYSTEM DESIGNS

With MoorDyn's verified polymer spring modeling, mooring systems featuring polymer springs can be designed and analyzed. The floating wind turbine used in this study is the VolturnUS-S semisubmersible with the International Energy Agency 15-MW reference wind turbine [9]. We modified the original catenary chain mooring system of the VolturnUS-S design for site conditions in the New York Bight area with a 50-m water depth to form the baseline design. We then modified the baseline design to include polymer springs. The following sections outline the load cases, simulation settings, and mooring design details.

3.1 Environmental Conditions and Simulation Settings

We designed the mooring systems to site conditions appropriate for the New York Bight area. Two design-driving conditions were chosen for OpenFAST simulations of the mooring systems: an operational case at rated wind speeds with the maximum operational sea state and a parked case with extreme 50-year-storm conditions. The former case represents the most extreme forces acting on an operating turbine, whereas the latter represents the worst wind and wave conditions over a 50-year statistical return period with a parked turbine. Table 2 summarizes the properties for each design load case (DLC).

TABLE 2: DESIGN-DRIVING LOAD CASES SUMMARY

Case Type	Normal	50 Year
Turbine status	Operating	Parked
International Electrotechnical Commission design load case	1.6	6.1a
Return period (yr)	50	50
Wind speed (m/s)	10.59	41.10
Turbulence intensity	0.085	0.154
Significant wave height (m)	4.72	8.70
Wave period (s)	10.03	12.73
Peak-shape parameter	2.02	2.03

Figure 4 depicts the baseline mooring system with wind and wave headings shown. The 0° wind-wave heading is expected to produce peak line tensions, with mooring line 2 directly upwind. Cases with 30° and 90° wind-wave headings are also checked for yaw stability.

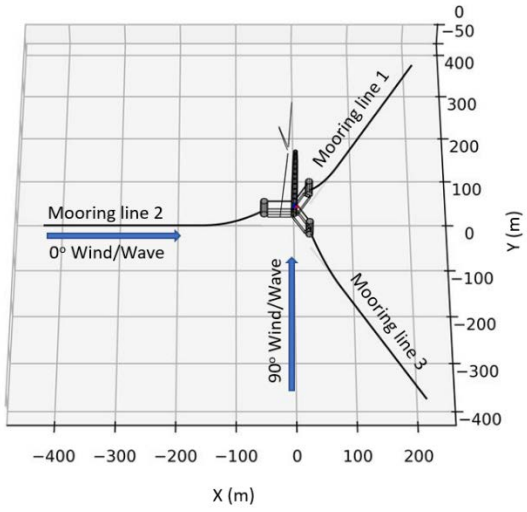

FIGURE 4: MOORING SYSTEM DIAGRAM

The simulations are 1 hour and 10 minutes long, with the first 10 minutes excluded from statistical calculations to allow for transients to dissipate. The MoorDyn setup uses a discretization of 35 segments for the chain lines and 6 segments for the springs. TurbSim was used to generate turbulent inflow wind, with a grid size of 290 m high by 250 m wide, with a 15-m grid spacing. Additional OpenFAST time step parameters are reported in Table 3.

TABLE 3: OPENFAST SIMULATION PARAMETERS

Simulation Parameter	Value
Simulation length	4200 s
Transient time	600 s
OpenFAST time step	0.025 s
MoorDyn time step	0.001 s
ElastoDyn time step	0.025 s
HydroDyn time step	0.25 s
TurbSim time step	0.05 s

3.2 Baseline Mooring Design

The baseline mooring system was based on the UMaine VolturnUS-S reference design, using the specified chain diameter of 185 mm [9]. This mooring design provides a simple basis for understanding the dynamic effects of the polymer spring. The mooring system was adjusted for a 50-m water depth using a line optimization method that minimizes cost for a specified offset. The specified offset and resulting pretension were adjusted to maintain yaw stiffness in off-angle wind-wave headings while keeping peak tensions low. The resulting design has an anchor radius of 431 m, a line length of 381 m, and a pretension of 1076 kN. Table 4 shows the parameters for the baseline design.

3.3 Spring-Equipped Mooring Design

We designed the spring-equipped mooring system to be consistent with the baseline mooring system, except for the addition of a polymer spring to each mooring line. The diameter of the chain could be reduced due to the tension reduction from the polymer springs, but in this study the diameter of the chain was kept consistent to show a clear and simple picture of the effects of the polymer springs. Figure 5 depicts the behavior of the polymer spring, showing how its nonlinear tension-strain curve results in load reductions compared to a linear spring. For typical motions around the mean tension, the spring behaves like a chain with a linear tension-strain curve. However, for extreme motions, the spring allows more elongation than chain and therefore reduces the tension increase. The spring rating is equal to the tension at the bend of the stress-strain curve. The optimal spring sizing will have a maximum load that is slightly below the spring rating. A spring sized too large will have extreme tensions that stay in the lower, steeper region of the curve, underutilizing the spring's ability to reduce tensions. A spring sized too small may have tensions that surpass the bend of the stress-strain curve, resulting in large and abrupt loads in the spring structure.

The nonlinear tension-strain curve of the polymer springs has a large impact on the tension-offset curve for the mooring line. Figure 6 shows the fairlead tension as a function of horizontal displacement along the mooring line heading for the baseline and spring-equipped designs. The designs show a similar fairlead tension up to a displacement of 1 m. Beyond 1 m, the baseline mooring design shows a steep nonlinear force as displacement increases due to the chain lifted off the seabed. The spring-equipped design shows a much lower tension with increased displacement, as the spring stretches to compensate for the offset.

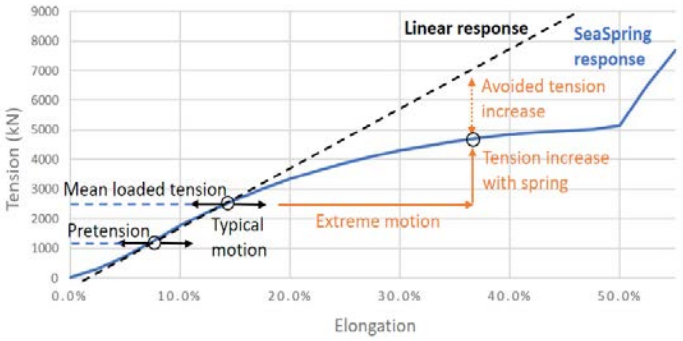

FIGURE 5: SIZING AND EXTREME TENSION REDUCTION FROM POLYMER SPRING

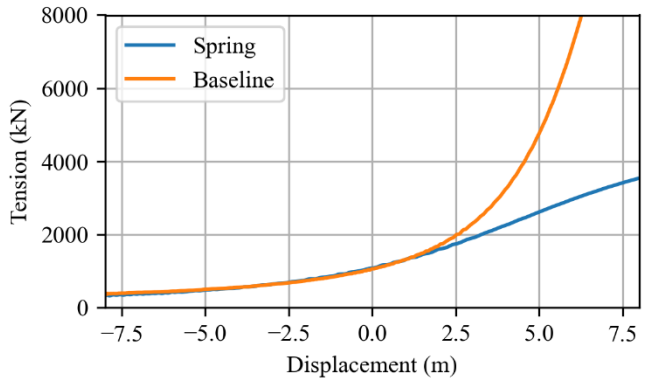

FIGURE 6: FAIRLEAD TENSION-DISPLACEMENT CURVE FOR THE BASELINE AND SPRING-EQUIPPED MOORING DESIGNS

The spring-equipped mooring design has the same chain diameter and anchor spacing as the baseline design but has polymer springs connected at the fairlead of each line. The polymer spring was initially sized using the ultimate limit state (ULS) load observed in the baseline design, of around 8 MN. We iterated the spring rating based on the updated ULS load observed in simulations of the spring-equipped design, until reaching a spring size that is only slightly higher than the ULS load. The final spring is rated at 4 MN for a ULS load of 3.3 MN. The stress-strain curve for the spring at this final sizing is shown in Figure 7. The spring length was also varied. With shorter springs, there is little room for elongation and the impact on tensions is minimal. With longer springs, the strain on the spring results in a large elongation, causing extreme platform surge motions. The tension and platform surge impacts were balanced to find a spring length with advantageous tension reductions and acceptable platform offsets. The chosen spring length is 17.6 m, approximately two times the significant wave height in the 50-year-storm conditions. Finally, the length of the chain was varied to maintain the same pretension as the baseline design for fair comparison. The polymer springs have a lighter weight in water than chain due to the large diameter, so the chain was tightened to increase tension. The resulting chain line length in the spring-equipped design is 361.8 m.

Figure 1 depicts a rendering of a sample mooring line with three polymer springs at the fairlead, but in the spring-equipped design for this study, only a single spring is used. In the MoorDyn model, the springs are attached directly to the platform and the spring padeyes are not modeled, but the padeye weight is included in the spring mass. The properties of the spring-equipped mooring design are summarized in Table 4.

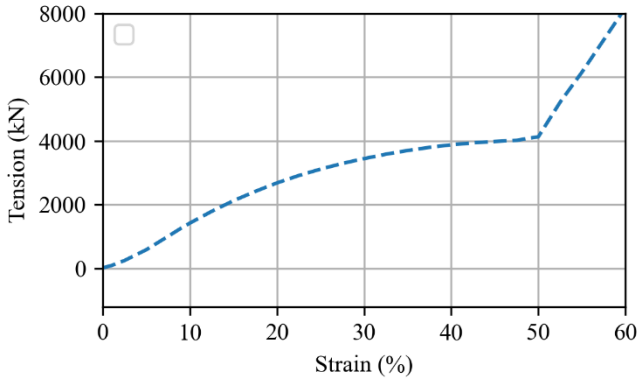

FIGURE 7: STRESS-STRAIN RESPONSE CURVE FOR THE SPRING-EQUIPPED MOORING DESIGN (4000 KN V3LR25 SPRING)

TABLE 4: BASELINE AND SPRING-EQUIPPED MOORING DESIGN PROPERTIES

	Baseline	Spring
Anchor radius (m)	431.3	431.3
Line length (m)	381.3	361.8
Line diameter (mm)	185.0	185.0
Line linear mass (kg/m)	681.1	681.1
Spring length (m)	-	17.6
Spring diameter (mm)	-	1.43
Spring linear mass (kg/m)	-	1759.9
Spring capacity (kN)	-	4000
Pretension (kN)	1076	1076

4. RESULTS AND DISCUSSION

To evaluate the behavior of polymer springs in shallow-water mooring systems, we simulated the baseline and spring-equipped mooring designs in OpenFAST for the design-driving load cases. This section presents results for the dynamic analysis of the baseline and spring-equipped mooring designs in normal operating and 50-year-storm environmental conditions.

4.1 Performance in Normal Operating Conditions

The baseline and spring-equipped mooring designs were simulated in normal operating conditions to understand the impact of the polymer springs on an operating wind turbine in severe waves. Figure 8 compares the platform motions for the baseline and spring-equipped designs in normal operating conditions. The surge time series shows a higher mean surge for

the spring-equipped design, as the spring allows more elongation to keep tensions down. The oscillations in surge are similar between the two designs. Similarly, the pitch time series shows slightly higher peaks in the spring-equipped design. Table 5 shows the mean and maximum platform surge in the baseline and spring-equipped designs. The addition of polymer springs increases mean surge by 53% and maximum surge by 48%. However, the baseline design is relatively stiff, with low surge values, so the mean and maximum surge values in the spring-equipped design of 5.2 m and 7.5 m are still reasonable from a design perspective. When adding polymer springs to a real mooring design, the pretension on the mooring lines could be increased to reduce the turbine watch circle. This increased pretension would somewhat limit the load reduction benefits and this trade-off can be optimized to yield the most cost-effective design.

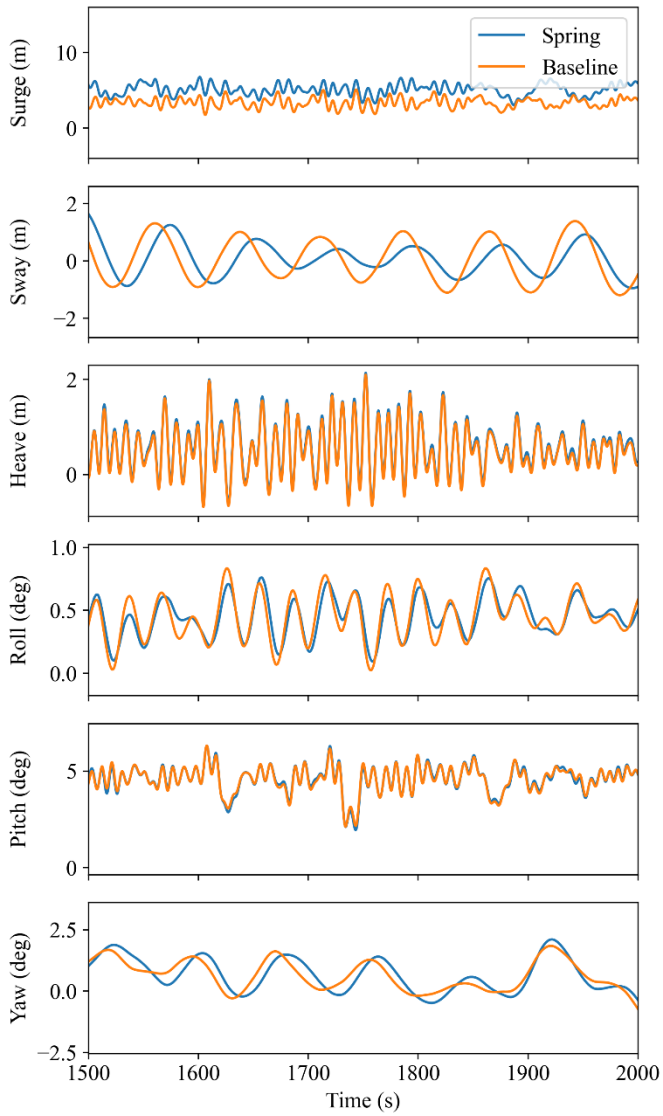

FIGURE 8: PLATFORM MOTIONS IN NORMAL OPERATING CONDITIONS

The platform motions in off-angle wind-wave headings were also checked to ensure that the spring-equipped design maintains reasonable platform motions. Earlier design iterations with lower pretensions were prone to large yaw motions in some environmental headings. We mitigated the large yaw motions by increasing the pretension in the mooring systems. For the final designs, the platform yaw angle stays below 5° in 30° and 90° wind-wave headings.

Figure 9 shows the line tensions for the baseline and spring-equipped designs in normal operating conditions. The tensions are measured at the fairlead connection, as it is assumed that the spring-equipped design would have chain connecting the spring to the platform. The downwind lines 1 and 3 show a lower average tension in the spring-equipped design but the amplitude of oscillations is similar. Mooring line 2, the directly upwind line, shows a similar mean tension in both designs but clearly higher peak tensions in the baseline design. These observations are further supported by the statistics in Table 5. The mean tensions in the downwind lines are approximately 10% lower in the spring-equipped design, with maximum tensions that are 3%-4% lower. The mean tension in the upwind line is only 3% lower in the spring-equipped design, but maximum tensions are 24% lower.

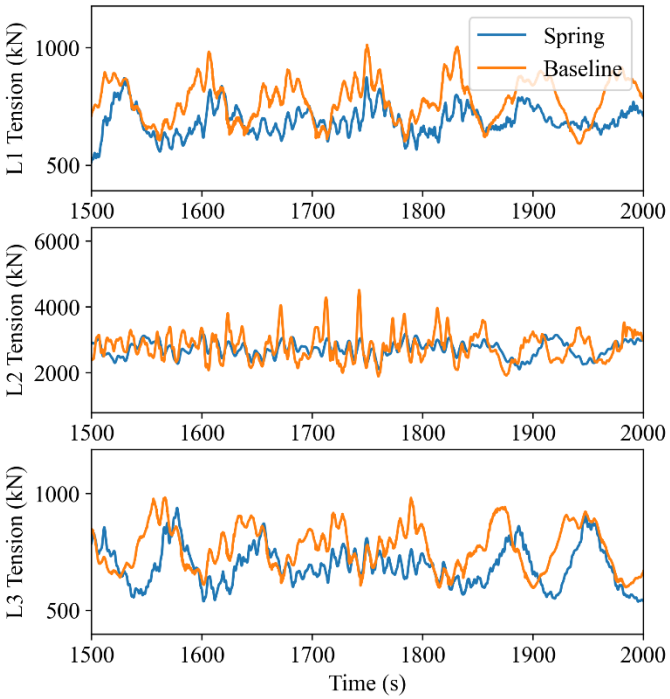

FIGURE 9: LINE TENSIONS IN NORMAL OPERATING CONDITIONS

TABLE 5. STATISTICS OF PLATFORM SURGE AND LINE TENSIONS FOR NORMAL OPERATING CONDITIONS

	Baseline	Spring	% Change
Mean surge (m)	3.4	5.2	53%
Maximum surge (m)	5.1	7.5	48%
L1 mean tension (kN)	762	683	-10%
L1 maximum tension (kN)	1088	1054	-3%
L2 mean tension (kN)	2811	2740	-3%
L2 maximum tension (kN)	4506	3405	-24%
L3 mean tension (kN)	767	686	-11%
L3 maximum tension (kN)	1154	1104	-4%

The advantage of the tension peak reductions is shown in the damage equivalent loads (DELs) in Table 6. The damage equivalent loads are again measured at the fairlead connection, as it will have the highest tensions, and are calculated using a fatigue slope of 5. The DELs in the downwind lines are very low in both the baseline and spring-equipped design. The upwind line, however, has a baseline DEL that is about eight times higher than the downwind lines. In the simulated load case, the spring-equipped design reduces the upwind DEL by 46%. The majority of damage will accumulate when a mooring line is in a fully loaded, upwind condition, so these results clearly show that the polymer springs improve fatigue life for this mooring system.

TABLE 6: DAMAGE EQUIVALENT LOADS IN NORMAL OPERATING CONDITIONS

	Baseline	Spring	% Change
L1 DEL (kN)	143	160	12%
L2 DEL (kN)	1054	571	-46%
L3 DEL (kN)	151	158	4%

Figure 10 shows the power spectral density (PSD) of platform surge in the baseline and spring-equipped designs. As shown in the plot, the surge PSDs for the baseline and spring-equipped designs match up very closely. This analysis indicates that the addition of polymer springs does not introduce additional resonant frequencies in the platform surge. In the lower plot, Figure 10 shows the PSD of the upwind line tension. The spring-equipped design's tension PSD generally exceeds the baseline design. At higher frequencies, the spring-equipped design shows some PSD peaks that do not appear in the baseline design. The high-frequency peaks appear to be multiples of the wave frequency. More investigation should be done to understand the PSD of the spring-equipped design's upwind line tension.

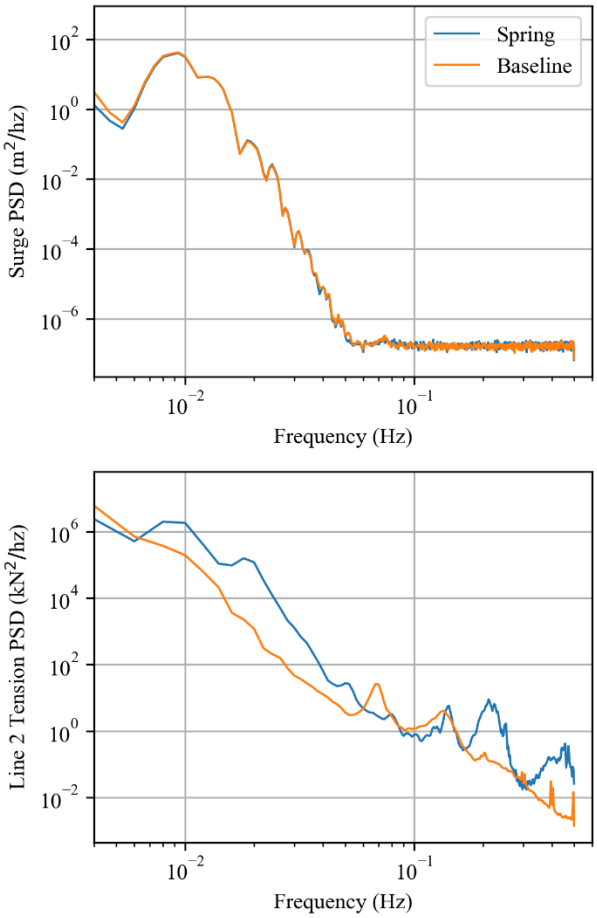

FIGURE 10: PSD OF PLATFORM SURGE AND UPWIND LINE TENSION IN NORMAL OPERATING CONDITIONS

4.2 Performance in 50-Year-Storm Conditions

We evaluated the baseline and spring-equipped designs in the 50-year-storm load case to characterize the behavior in the worst wind and wave conditions over a 50-year statistical return period. The platform motions for the baseline and spring-equipped design are shown in Figure 11. Both designs have a lower average surge in the 50-year-storm conditions because the wind turbine is parked with the blades pitched to reduce the thrust force as much as possible. Similar to the results for the normal load case, the spring-equipped design shows higher peak surge motions. The statistics in Table 7 show that the spring-equipped design has a 36% higher mean surge and a 14% higher maximum surge.

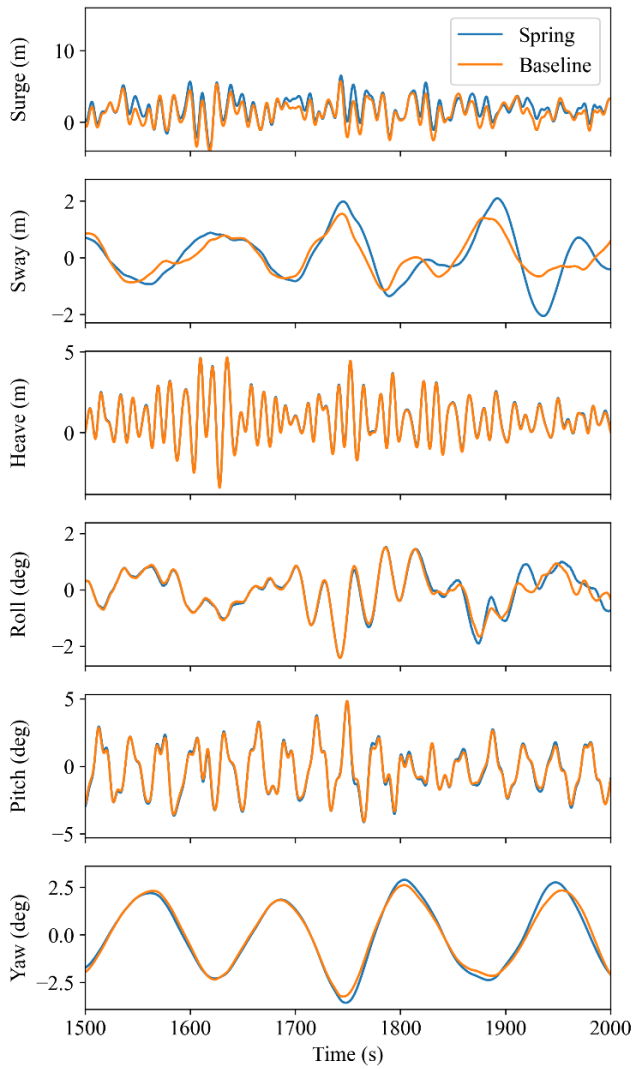

FIGURE 11: PLATFORM MOTIONS IN THE 50-YEAR-STORM CONDITIONS

The line tensions from the 50-year storm load case are shown in Figure 12. All three lines show similar mean tensions between the baseline and spring-equipped designs. The downwind lines show close agreement in tensions, with the same phase and mean tensions. The upwind line tension also shows the same phase between the two designs; however, the baseline peak tensions are much higher. The reduction in peak tension seen in the spring-equipped design depends on the magnitude of the tension. As shown in the time series, the smaller peaks show tension reductions of about 10%–20%. The larger peak tensions in the baseline design, like at around 1750 s, show tension reductions of 60%. The larger tensions in the baseline design benefit the most from the shape of the spring curve, with reductions that are in the most compliant region near the elbow of the curve.

When the peak tension at 1750 s occurs, the spring-equipped design has approximately 80 m more chain on the seabed than the baseline design. This supports the conclusion that the polymer spring elongates to accommodate platform offsets in the spring-equipped design while the chain must lift off the seabed in the baseline design, resulting in large tensions. This difference can be leveraged for cost reduction by decreasing the anchor spacing and chain length in polymer spring-equipped mooring designs.

The line tension statistics in Table 7 further support the conclusion that the spring-equipped design reduces maximum tensions. The mean tensions are within 3% across the three lines. The downwind lines show more mild reductions in maximum tension of 6%–18%, whereas the upwind line reveals a maximum tension reduction of 59%. The advantage of the maximum line tension reductions is shown in the DELs calculated in Table 8. The spring-equipped design reduces the DEL in the downwind lines in the 50-year-storm conditions by 40%. The upwind line shows an even larger reduction in DEL of 55%.

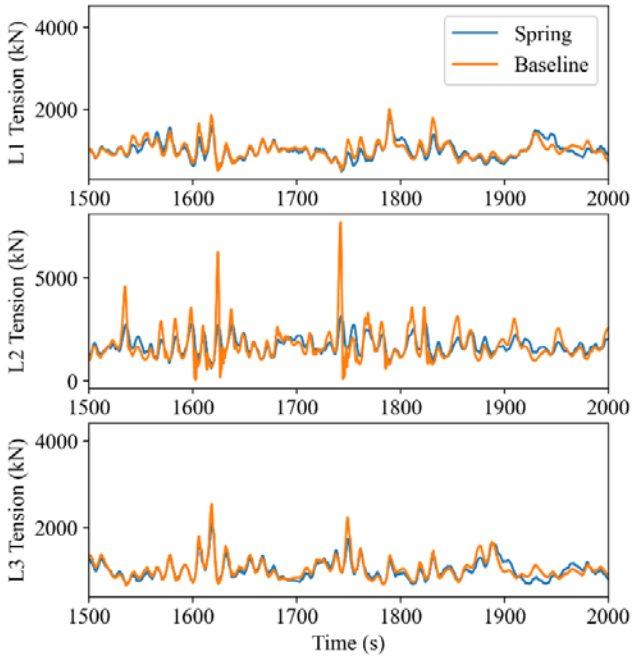

FIGURE 12: LINE TENSIONS IN THE 50-YEAR-STORM CONDITIONS

TABLE 7: STATISTICS OF PLATFORM SURGE AND LINE TENSIONS IN THE 50-YEAR-STORM CONDITIONS

	Baseline	Spring	% Change
Mean surge (m)	1.4	1.9	36%
Maximum surge (m)	5.7	6.5	14%
L1 mean tension (kN)	1009	983	-3%
L1 maximum tension (kN)	2010	1880	-6%
L2 mean tension (kN)	1683	1677	0%
L2 maximum tension (kN)	7713	3155	-59%
L3 mean tension (kN)	1020	1007	-1%
L3 maximum tension (kN)	2537	2089	-18%

TABLE 8. DAMAGE EQUIVALENT LOADS IN THE 50-YEAR STORM CONDITIONS

	Baseline	Spring	% Change
L1 DEL (kN)	722	435	-40%
L2 DEL (kN)	1798	802	-55%
L3 DEL (kN)	687	421	-39%

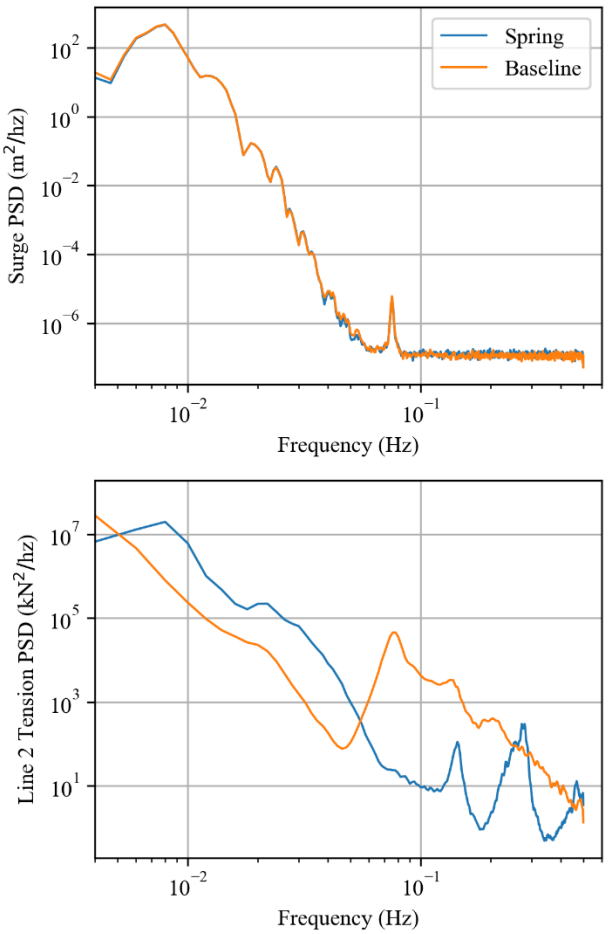

FIGURE 13: PSD OF SURGE AND UPWIND LINE TENSION IN THE 50-YEAR STORM CONDITIONS

Figure 13 shows the PSD plots of platform surge and upwind line tension in the 50-year-storm conditions. The surge PSD matches closely between the two designs, showing that while the spring-equipped design allows slightly more surge, it does not introduce an additional surge natural frequency. The tension PSD shows higher tension excitation in the spring-equipped design at frequencies below 0.05 Hz. At around 0.08 Hz, which corresponds to the peak period of the waves, the baseline design shows a clear peak in the PSD while the spring-equipped design does not. The polymer springs act to ease the tension spikes caused by waves. Similar to the result seen in the normal operating case, the spring-equipped design shows some high-frequency peaks in the line tension PSD that do not match the baseline design. The increased PSD in the spring design may be a result of modeling limitations, as the springs—in reality—would have a small amount of damping that would likely reduce the modal response shown in the PSD. More investigation into the tension PSD should be done to understand these differences.

5. CONCLUSION

In this study, we explored the effect of polymer springs in a shallow-water floating wind turbine mooring system. A capability for modeling the nonlinear tension-strain response of polymer springs was added to MoorDyn and verified against OrcaFlex simulations, with very good agreement. The original mooring system of the VolturnUS-S semisubmersible floating wind turbine was adapted to suit a 50-m water depth. With the new MoorDyn capability, a mooring system featuring polymer springs was designed and analyzed to show the effects of polymer springs on key dynamic behaviors. Using a baseline design without polymer springs as a basis for comparison, we analyzed the line tensions and platform motions in design-driving load cases to understand the dynamic impacts of polymer springs.

In normal operating conditions, the addition of polymer springs reduces peak loads by up to 24% while allowing slightly larger platform offsets. The platform surge motions are increased by about 50%, but these motions stay within a maximum surge of 7.2 m, a reasonable offset for cable considerations. The DELs show minimal change in the downwind lines, but the upwind line DEL in normal operating conditions is reduced by 46%. In the 50-year-storm load case, the tension reductions in the spring-equipped design are more extreme: up to a 60% reduction in peak loads for the upwind line. There is also a significant reduction in how much mooring line is lifted off the seabed. These results show that for a catenary mooring system at a 50-m water depth, polymer springs significantly reduce peak line tensions and line liftoff from the seabed, raising the possibility of cost savings from reduced chain diameters and mooring line lengths.

In this study, we did not reduce the diameter of chain in the spring-equipped design so the impact on mooring system cost would be minimal. However, these results clearly show the potential for polymer springs to reduce overall mooring system loads. Future studies should explore leveraging polymer springs to reduce mooring component sizes and resulting mooring system costs. Additionally, future work should analyze the effects of polymer springs on alternative mooring designs, like semi-taut systems with rope lines.

ACKNOWLEDGEMENTS

This work was authored by the National Renewable Energy Laboratory, operated by Alliance for Sustainable Energy, LLC, for the U.S. Department of Energy (DOE) under Contract No. DE-AC36-08GO28308. Funding was provided by the National Offshore Wind Research and Development Consortium for the project “Technical Qualification and Commercial Assessment of Innovative Shallow Water Mooring Components for Floating Wind Platforms.” The views expressed in the article do not

REFERENCES

[1] W. Musial and B. Ram, "Large-Scale Offshore Wind Power in the United States: Assessment of Opportunities and Barriers," *National Renewable Energy Laboratory*, Jan. 2010, doi: 10.2172/990101.

[2] A. Campanile, V. Piscopo, and A. Scamardella, "Mooring design and selection for floating offshore wind turbines on intermediate and deep water depths," *Ocean Engineering*, vol. 148, pp. 349–360, Jan. 2018, doi: 10.1016/j.oceaneng.2017.11.043.

[3] W. Hsu, K. P. Thiagarajan, M. Hall, M. MacNicoll, and R. Akers, "Snap Loads on Mooring Lines of a Floating Offshore Wind Turbine Structure," Volume 9A: Ocean Renewable Energy, Jun. 2014. doi: 10.1115/OMAE2014-23587.

[4] K. Xu, K. Larsen, Y. Shao, M. Zhang, Z. Gao, and T. Moan, "Design and comparative analysis of alternative mooring systems for floating wind turbines in shallow water with emphasis on ultimate limit state design," *Ocean Engineering*, vol. 219, p. 108377, Jan. 2021, doi: 10.1016/j.oceaneng.2020.108377.

[5] W.-H. Huang and R.-Y. Yang, "Water Depth Variation Influence on the Mooring Line Design for FOWT within Shallow Water Region," *Journal of Marine Science and Engineering*, vol. 9, no. 4, 2021, doi: 10.3390/jmse9040409.

[6] M. J. Harrold, P. R. Thies, P. Halswell, L. Johanning, D. Newsam, and C. Bittencourt Ferreira, "Demonstration of the Intelligent Mooring System for Floating Offshore Wind Turbines," ASME 2019 2nd International Offshore Wind Technical Conference, Nov. 2019. doi: 10.1115/IOWTC2019-7544.

[7] P. McEvoy, S. Kim, and M. Haynes, "Fibre Spring Mooring Solution for Mooring Floating Offshore Wind Turbines in Shallow Water," Volume 9: *Ocean Renewable Energy*, Jun. 2021. doi: 10.1115/OMAE2021-62892.

[8] M. Hall and A. Goupee, "Validation of a lumped-mass mooring line model with DeepCwind semisubmersible model test data," *Ocean Engineering*, vol. 104, pp. 590–603, Aug. 2015, doi: 10.1016/j.oceaneng.2015.05.035.

[9] C. Allen *et al.*, "Definition of the UMaine VolturnUS-S Reference Platform Developed for the IEA Wind 15-Megawatt Offshore Reference Wind Turbine," National Renewable Energy Laboratory (NREL), Golden, CO (United States), NREL/TP-5000-76773, Jul. 2020.